



HHS Public Access

Author manuscript

Oral Surg Oral Med Oral Pathol Oral Radiol. Author manuscript; available in PMC 2018 August 09.

Published in final edited form as:

Oral Surg Oral Med Oral Pathol Oral Radiol. 2018 June ; 125(6): 670–681. doi:10.1016/j.oooo.2018.02.020.

Noninvasive diagnostic adjuncts for the evaluation of potentially premalignant oral epithelial lesions: current limitations and future directions

Eric C. Yang, BS^{a,b}, Melody T. Tan, MSE^a, Richard A. Schwarz, PhD^a, Rebecca R. Richards-Kortum, PhD^a, Ann M. Gillenwater, MD^c, and Nadarajah Vigneswaran, BDS, DrMedDent, DMD^d

^aDepartment of Bioengineering, Rice University, Houston, TX, USA

^bMedical Scientist Training Program, Baylor College of Medicine, Houston, TX, USA

^cDepartment of Head and Neck Surgery, M.D. Anderson Cancer Center, University of Texas, Houston, TX, USA

^dDepartment of Diagnostic and Biomedical Sciences, University of Texas School of Dentistry, Houston, TX, USA

Abstract

Potentially premalignant oral epithelial lesions (PPOELs) are a group of clinically suspicious conditions, of which a small percentage will undergo malignant transformation. PPOELs are suboptimally diagnosed and managed under the current standard of care. Dysplasia is the most well-established marker to distinguish high-risk PPOELs from low-risk PPOELs, and performing a biopsy to establish dysplasia is the diagnostic gold standard. However, a biopsy is limited by morbidity, resource requirements, and the potential for underdiagnosis. Diagnostic adjuncts may help clinicians better evaluate PPOELs before definitive biopsy, but existing adjuncts, such as toluidine blue, acetowhitening, and autofluorescence imaging, have poor accuracy and are not generally recommended. Recently, *in vivo* microscopy technologies, such as high-resolution microendoscopy, optical coherence tomography, reflectance confocal microscopy, and multiphoton imaging, have shown promise for improving PPOEL patient care. These technologies allow clinicians to visualize many of the same microscopic features used for histopathologic assessment at the point of care.

Over 300,000 new cases of oral cancer are diagnosed annually worldwide, with particularly high incidence rates in South and Southeast Asia, Europe, Latin America, and the Caribbean and Pacific nations. Risk factors for oral cancer include tobacco use, excessive consumption of alcohol, and betel quid chewing. The 5-year survival rate for oral cancers is only about

This is an open access article under the CC BY-NC-ND license (<http://creativecommons.org/licenses/by-nc-nd/4.0/>).

Reprint requests: Nadarajah Vigneswaran, BDS, DrMedDent, DMD, University of Texas School of Dentistry, Department of Diagnostic and Biomedical Sciences, 7500 Cambridge Street, Houston, TX 77054, USA, nadarajah.vigneswaran@uth.tmc.edu.

R. Richards-Kortum and A. M. Gillenwater are recipients of licensing fees for intellectual property licensed from the University of Texas at Austin by Remicalm LLC.

50%, largely because oral cancers are most commonly diagnosed in advanced stages of disease.^{1,2}

Oral cancers are typically preceded by potentially premalignant oral epithelial lesions (PPOELs), a group of clinically suspicious conditions, including leukoplakia, erythroplakia, submucous fibrosis, and lichen planus.³ Although the majority of PPOELs do not progress to cancer, distinguishing high-risk PPOELs from low-risk PPOELs is difficult. As a result, under the current standard of care, PPOELs are suboptimally diagnosed and managed. In this article, we will discuss the limitations of the existing methods of PPOEL risk assessment, including biopsy and noninvasive diagnostic adjuncts. Then, we will introduce in vivo microscopy (IVM), a novel group of technologies that could help clinicians overcome these limitations by allowing them to visualize microscopic, histology-like features of PPOELs at the point of care.

DYSPLASIA AS A MARKER FOR MALIGNANT PROGRESSION

The most widely accepted marker to assess the risk of a PPOEL eventually undergoing malignant transformation is the presence and grade of dysplasia in the lesion. *Dysplasia* is defined as the presence of specific epithelial architectural and cytologic changes and is graded as mild, moderate, or severe based on the depth and severity of the changes. It is frequently assumed that oral carcinogenesis involves PPOELs that undergo a gradual progression beginning with hyperplasia and evolving through stages of mild dysplasia, moderate dysplasia, severe dysplasia, carcinoma in situ (CIS), and finally carcinoma after cellular invasion through the basement membrane. In reality, it is likely that in some cases, the course of oral cancer does not occur in such an orderly manner. PPOELs with dysplasia are considered non-obligate precursors of oral squamous cell carcinoma (OSCC), indicating that not all dysplastic PPOELs will progress to invasive cancer.

PPOELs containing dysplasia are more likely to undergo malignant transformation, and the risk increases as the grade of dysplasia increases. One recent meta-analysis estimated the malignant transformation rate of all leukoplakia, regardless of dysplasia, at 3.4%, with results of individual studies ranging from 0.13% to 34.0%.⁴ Lesions containing dysplasia have a higher transformation rate. Bouquot et al.⁵ estimated that less than 5% of mild dysplasia cases undergo eventual malignant transformation compared with 3% to 15% for moderate dysplasia and 16% (range 7%–50%) for severe dysplasia or CIS. A 2009 meta-analysis estimated the transformation rate as 12.1% (confidence interval [CI] 8.1%–17.9%) for dysplastic lesions with a 10.3% rate (CI 6.1%–16.8%) for mild to moderate dysplasia and 24.1% (CI 13.3%–39.5%) for severe dysplasia and CIS.⁶ Differences in patient population and interobserver variation in diagnosis, treatment, and follow-up likely account for the inconsistent estimates.

Despite ubiquitous use, dysplasia is an imperfect risk marker because at its core, carcinogenesis is driven by the accumulation of somatic mutations and epigenetic changes. The relationship between these key drivers of carcinogenesis and the dysplasia phenotype is unclear.⁷ Reports of OSCC arising from nondysplastic mucosal areas, the presence of genetic alterations in histologically normal epithelium adjacent to carcinoma, and the high

recurrence rates after retinoic acid-induced regression of dysplasia provide evidence for the phenotype–genotype disparity.^{8–10} Thus, much effort has been devoted to the discovery of molecular biomarkers capable of distinguishing progressive PPOELs from nonprogressive PPOELs (reviewed elsewhere in this focus issue). Although genetic loss of heterozygosity is considered a better marker for predicting the malignant progression risk of a PPOEL, it has not been integrated into day-to-day clinical practice.¹¹ A number of studies have attempted to identify biomarkers to predict which patients are likely to develop OSCC after the diagnosis of PPOEL with dysplasia, but so far, no such biomarkers have been validated and prospectively shown to predict malignant transformation risk. Therefore, the degree of dysplasia will remain the key determinant for assessing the malignancy risk of PPOELs until emerging biomarkers are validated and integrated into clinical use.

TISSUE BIOPSY IS REQUIRED TO DIAGNOSE DYSPLASIA

The current clinical gold standard for predicting the cancer progression risk of a PPOEL requires biopsy and microscopic evaluation of the resulting hematoxylin-and-eosin (H&E)–stained tissue section by a trained oral and maxillofacial or head and neck pathologist to determine the presence and grade of dysplasia or carcinoma. Conventional oral examination (COE) alone is insufficient for risk stratification. COE is generally effective for lesion identification, but not for the ensuing clinical workup for treatment planning. Once an oral lesion has been discovered, it must be classified as a PPOEL or a nonsuspicious lesion, a distinction that many general dental practitioners (GDPs) are not sufficiently trained to make.¹² Seoane et al.¹³ assessed 32 GDPs in Northwestern Spain by showing them photographs of 50 oral mucosal lesions, including 31 benign lesions, 12 PPOELs, and 7 cases of OSCC. The GDPs distinguished OSCC and PPOELs from benign lesions with only 57.8% sensitivity and 53% specificity, a result only marginally better than random guessing. Specialists are likely more capable of distinguishing PPOELs from nonsuspicious lesions.¹²

Once a lesion has been classified as a PPOEL, classifying it as dysplastic or nondysplastic based on COE is extremely difficult regardless of training level. A 2012 meta-analysis estimated that COE had 93% sensitivity but only 31% specificity for the identification of dysplasia or carcinoma.¹⁴ Most of the studies had been performed in specialty clinics, and inclusion criteria ranged from including only PPOELs and OSCC to including any oral mucosal lesion. More recently, a retrospective analysis of 1003 oral lesions at a tertiary medical center found that oral and maxillofacial surgeons distinguished dysplastic or cancerous lesions from benign lesions with a sensitivity of 48.6% and specificity of 98.1%.¹⁵ These studies demonstrated the ineffectiveness of COE for PPOEL risk stratification, although the specific balance of sensitivity and specificity may vary, in part, as a result of differences in the definition of a positive COE.

LIMITATIONS OF BIOPSY

Once the decision has been made to perform biopsy on a PPOEL, the clinician must select a biopsy site, which should represent the area of the lesion most likely to contain dysplasia or carcinoma. The presence and grade of dysplasia and invasive carcinoma frequently vary throughout a lesion, and dysplasia may even be present in clinically normal mucosal areas

outside its visible boundaries. Excisional biopsy can be performed for smaller lesions and could prevent sampling bias, but the risk of incomplete excision of malignant lesions exists and the procedure is excessively aggressive in the case of benign lesions. For these reasons, incisional biopsy is typically preferred, but it does not assess an entire lesion. This sampling bias can lead to underdiagnosis or misdiagnosis, particularly in cases of multifocal, large, or nonhomogeneous PPOELs.

Goodson et al.¹⁶ analyzed 152 patients with a single leukoplakic lesion treated with laser excision, a mean of 4.43 months after a preoperative incisional biopsy, and found that 50% of the incisional biopsy diagnoses were upgraded on the basis of the excised specimen. Chen et al.¹⁷ assessed 80 oral mucosal lesions and found that incisional biopsy missed 6 OSCC cases. Underdiagnosis of dysplasia was not specifically discussed. In the largest sampling bias study, Lee et al.¹⁸ retrospectively found that incisional biopsy underdiagnosed 29.5% of leukoplakic lesions in 200 patients who underwent surgical resection within 30 days of the initial incisional biopsy. In 11 of the 24 patients with a diagnosis of carcinoma after surgery, the initial diagnosis based on incisional biopsy was no dysplasia or mild dysplasia. The 42 patients who underwent multiple incisional biopsy procedures had a lower rate of underdiagnosis (11.9%). Additionally, the authors found higher rates of underdiagnosis in nonhomogeneous lesions than in homogeneous lesions. The authors defined *homogeneous leukoplakia* as a white lesion with a uniform flat thin appearance or a white lesion with shallow cracks within a smooth, wrinkled, or corrugated surface of constant texture. *Nonhomogeneous leukoplakia* was defined as an irregularly flat, nodular, or exophytic white or white and red lesion.

There are several other limitations associated with biopsy (Table I). Multiple steps are required to prepare the biopsy sample before it is suitable for microscopic diagnosis. A skilled specialist is required to perform the biopsy procedure properly, and a trained pathologist is required to interpret the histopathologic findings. These requirements make it necessary for care providers to follow up with patients for several days after their initial visit, limiting the use of biopsy in resource-poor clinical sites. Grading dysplasia is subjective and involves high levels of interobserver and intraobserver variance, even among oral and maxillofacial or head and neck pathology specialists.^{19,20} The 2017 World Health Organization criteria for dysplasia requires assessment of numerous subjective factors with no objective method to weigh them.²¹ Discrepancies are particularly common with regard to cases of PPOELs diagnosed with mild dysplasia because of the difficulty in distinguishing mild dysplasia from reactive and reparative atypia associated with inflammation and ulcerations, respectively. Finally, invasive biopsy is associated with morbidity and cost.

EXISTING DIAGNOSTIC ADJUNCTS

The limitations discussed above have motivated ongoing attempts to develop diagnostic adjuncts to assist with PPOEL evaluation. In particular, there is a clinical need for diagnostic adjuncts that can augment COE to (1) help clinicians decide which lesions need biopsy by distinguishing high-risk PPOELs that harbor dysplasia or cancer from low-risk PPOELs and other mucosal lesions; (2) identify the highest risk sites within a PPOEL for biopsy guidance; and (3) longitudinally monitor PPOELs to decide if repeat biopsy procedures are

necessary. At present, diagnostic adjuncts should not replace COE—biopsy of PPOELs with sufficient clinical suspicion is recommended regardless of results obtained from adjuncts, nor should they replace biopsy for definitive diagnosis. The ideal diagnostic adjunct would provide accurate correlation with dysplasia and cancer, provide results immediately at the point of care, and evaluate a large area for biopsy guidance. Additionally, the diagnostic adjunct should be minimally-invasive, involve low cost, require few consumables, require minimal training to use, and allow objective interpretation. Common diagnostic adjuncts include toluidine blue, brush biopsy with cytology, acetowhitening with chemiluminescence, and autofluorescence imaging. Numerous authors have reviewed the evidence on these adjuncts,^{22–24} so we only briefly discuss them in the context of above criteria (Table II).

Use of the vital dye toluidine blue consists of an initial rinse of the oral cavity with acetic acid followed by toluidine blue. It is thought that the dye has an affinity for DNA, so increased DNA levels seen in dysplasia and carcinoma lead to greater staining.²⁵ Toluidine blue is low cost, provides immediate results, and can be used to assess the entire oral cavity but is limited by false positive results for inflammatory lesions or ulcers, low sensitivity for dysplasia, and subjective interpretation. An oral biopsy brush can be used to remove transepithelial cells with minimal invasion, and the cells are transferred to a slide and evaluated cytologically. Cytologic smears can then be evaluated for cellular atypia. When performed properly, brush biopsy is potentially the most accurate adjunct. A meta-analysis of cytology reported sensitivity and specificity of 91%.²⁴ However, brush biopsies can only assess a small region of the oral mucosa, do not provide results for days, and are not reliable for evaluating PPOELs with thick keratin layers. Acetowhitening entails rinsing the oral cavity with acetic acid and then using a chemiluminescent light to look for mucosal areas with a white appearance indicating a PPOEL. This approach can assess large regions at the point of care, but studies have demonstrated poor sensitivity and specificity.^{26,27} ViziLite (Zila Pharmaceuticals Inc., Phoenix, AZ) is an example of an acetowhitening and chemiluminescence product.

Autofluorescence imaging (AFI) is based on the concept that dysplasia and cancer cause measurable changes in tissue autofluorescence, defined as fluorescence intrinsic to tissue. Epithelial fluorophores, such as nicotinamide adenine dinucleotide (NADH) and flavin adenine dinucleotide (FAD), and stromal fluorophores, such as collagen and elastin, are the primary contributors to autofluorescence in the normal oral mucosa. Dysplasia and cancer are typically accompanied by a large loss of green autofluorescence, along with a small increase in red autofluorescence. Certain changes, such as increased metabolism, increased nuclear area and pleomorphism, increased epithelial thickness, increased vascularization, breakdown of collagen cross-links, and production of fluorophores by bacteria, contribute to this effect.

Several AFI devices have become commercially available in the past decade, including the VELscope (LED Dental, Atlanta, GA), Identafi (StarDental-DentaleZ, Englewood, CO), and OralID (Forward Science, Stafford, TX). Clinical use typically involves illumination of the tissue with blue or violet light in a darkened room, allowing the clinician to visualize tissue autofluorescence. Normal mucosal areas appear bright, whereas suspicious areas exhibit loss of fluorescence and appear dark. Interestingly, loss of fluorescence frequently

extends beyond the visible borders of a lesion, and these extensions often harbor dysplasia and loss of heterozygosity.²⁸ A randomized controlled trial is underway to investigate whether AFI can be used to delineate margins during surgical resection of OSCC to reduce recurrence rates.²⁹

The advantages of AFI include high sensitivity for dysplasia and cancer, capability to assess large areas of the oral mucosa at the point of care, nonrequirement of consumables, and noninvasiveness. Commercially available systems rely on subjective interpretation of autofluorescence, but AFI offers the potential for more objective interpretation. Unfortunately, AFI is limited by false positive results. Lesions of various etiologies have different autofluorescent properties (Table III); most commonly, inflammatory benign lesions also often exhibit a loss of fluorescence. Keratin is autofluorescent,³⁰ and in the authors' experience, hyperkeratinized high-risk PPOELs such as proliferative verrucous leukoplakia may not show loss of fluorescence even in the presence of dysplasia or cancer. The VELscope is approved for use by the U.S. Food and Drug Administration as an adjunct to enhance the visualization of oral mucosal abnormalities but not as a tool for risk stratification. AFI may have clinical utility for risk assessment during longitudinal monitoring of patients with known high-risk PPOELs or previous history of cancer.

It is clear from the above discussion that no existing diagnostic adjunct meets all of the ideal criteria. The adjuncts that provide immediate results from large regions (toluidine blue, acetowhitening and chemiluminescence, and AFI) suffer from limited accuracy because they do not directly assess the microscopic features used to diagnose dysplasia and cancer. Brush biopsy allows for direct assessment of cellular atypia but provides delayed results from small regions. Accordingly, the most recent American Dental Association guidelines included a conditional recommendation against the use of cytologic adjuncts; autofluorescence imaging; tissue reflectance adjuncts, such as chemiluminescence; and vital staining adjuncts, such as toluidine blue, for the assessment of clinically evident lesions.²²

IN VIVO MICROSCOPY

In recent years, a class of optical imaging technologies known as IVM has emerged as a promising new class of diagnostic adjunct. IVM combines the strengths of existing adjuncts by enabling high-resolution, microscopic imaging of intact tissue for disease detection and diagnosis at the point of care.

IVM produces images of microscopic tissue features by measuring tissue optical properties, such as reflectance, scattering, absorption, and fluorescence emission, which are frequently altered in disease states. IVM has been proposed for a range of clinical applications, including disease diagnosis, disease risk stratification, longitudinal monitoring of patients, and surgical margin delineation. IVM instrumentation has been integrated into many form factors, such as endoscopes, catheters, needles, and benchtop devices, allowing for their use in a variety of anatomic locations. Currently, an IVM technique called *optical coherence tomography* (OCT) is the standard of care in ophthalmology for retinal imaging.³¹ IVM has also gained clinical use for coronary angiography, evaluation of Barrett's esophagus, and diagnosis of skin lesions.³²⁻³⁴ Each IVM technology measures different tissue optical

properties and offers different capabilities in parameters, such as imaging depth, resolution, field of view (FOV), and acquisition time. Additional considerations include cost, size, and need for exogenous contrast agents. The choice to use a specific IVM technology is determined by optimally balancing trade-offs in these parameters to meet the minimum performance requirements of the desired clinical application.

Development of IVM technologies for PPOEL evaluation is still at an early stage. Here, we discuss IVM approaches that have been reported so far (Table IV), including our own work.

Multimodal imaging

Our group has developed an IVM device called the *high-resolution microendoscope* (HRME).^{35,36} The HRME is an inexpensive fluorescence microscope contained in a small box with an attached flexible probe 0.79 mm in diameter (Figure 1A). The clinician uses a cotton-tipped applicator to apply proflavine, a vital fluorescent dye that stains cell nuclei, to the tissue of interest. The probe is then placed in gentle contact with the proflavine-stained mucosa to visualize the surface epithelial nuclei directly. The depth of analysis is estimated to be 20 to 50 μm ,^{37,38} although no conclusive studies have fully assessed this range. Once a good image is obtained, the clinician can depress a foot pedal to freeze the current frame and then save and process the image. Changes in nuclear morphology that are characteristic of oral dysplasia and cancer are evident in HRME images and are easily evaluated, with little training required to identify differences. Small, evenly spaced nuclei are seen in the HRME images of the normal mucosa and benign lesions (Figure 1B), whereas large, crowded, and irregularly shaped nuclei are seen in the HRME images of dysplastic or cancerous lesions (Figure 1C). To provide an objective result, we have developed an automated computer algorithm that identifies nuclei and calculates metrics that are correlated with dysplasia and cancer, such as the nuclear/cytoplasm ratio and the density of abnormal nuclei.

A limitation of the HRME is its small, 0.79-mm FOV. Because it is too time consuming to assess an entire lesion 0.79 mm at a time, the clinician must choose the most suspicious sites within a lesion to image. We propose the use of AFI for this initial localization. As previously discussed, the 2 major weaknesses of commercially available AFI systems are low specificity and subjective image interpretation. The low specificity could be overcome by using the HRME to image the nuclei at the high-risk sites identified by AFI. For objective image interpretation, we have developed a quantitative risk metric called the *normalized red/green* (RG) *ratio*, which can be automatically calculated from AFI images through a computer algorithm.³⁹ The normalized RG ratio of a pixel is equal to its red intensity divided by its green intensity, normalized by the value of the same ratio at a region of the normal mucosa. The purpose of normalization is to account for interpatient variation in the autofluorescence of the normal mucosa. Dysplasia and cancer decrease green autofluorescence and increase red autofluorescence, so an elevated normalized RG ratio is a marker of increased risk for malignancy. A study using this multimodal imaging approach combining AFI with the HRME was conducted on 100 sites in 30 patients at the MD Anderson Cancer Center (Houston, TX) immediately before surgical resection of an oral lesion. It was found that the combination of nuclear/cytoplasm ratio and the normalized RG

ratio correctly diagnosed 95% of patients with moderate dysplasia to cancer and 98% of normal sites (Figure 2). A reference standard of histopathology was performed for all sites.⁴⁰

The potential benefit of multimodal imaging can be illustrated by the case of a patient evaluated by one of the authors of this article (NV) at the University of Texas School of Dentistry (Houston, TX) as part of an institutional review board–approved protocol. The patient was a 75-year-old female with a chief complaint of tongue pain and soreness. She had previously been diagnosed with squamous cell carcinoma of the right lateral tongue 11 years before presentation and had been treated with partial glossectomy. A large, heterogeneous red-and-white ulcerated lesion (Figure 3A) involving the right ventral tongue and the floor of mouth was evident under visual examination. Biopsy of this ulcerated lesion had been performed at least 4 times at various clinics, all showing negative results for dysplasia or carcinoma, within 3 years of presentation. The lesion was first imaged with AFI (Figure 3B), which demonstrated loss of fluorescence subjectively and elevated normalized RG ratio objectively. The patient was then imaged with the HRME (Figure 3C), and abnormal nuclei (Figure 3D) were quickly found at a site with elevated normalized RG ratio. Biopsy of the imaging site revealed invasive OSCC, and the patient was referred to a head and neck surgical oncologist for further treatment. This patient had not been accurately diagnosed under the existing standard of care; it is likely that her previous biopsy specimens were not taken from the optimal location. Although it is possible that OSCC had not yet developed at the time of her previous biopsy procedures, this is less likely considering the heterogeneity of the lesion and that her previous biopsy results were negative for dysplasia. In contrast, multimodal imaging, at the point of care, was able to localize high-risk regions and noninvasively detect abnormal cells, which were confirmed to be malignant on biopsy.

As discussed, we have shown that combining the quantitative parameters from AFI and HRME images can help accurately diagnose high-grade dysplasia and cancer at imaged sites in a population with a high prevalence rate. However, we have not yet assessed the 2-step procedure of AFI for site localization followed by the HRME in a prospective, systematic way. A risk heat map based on AFI is one approach to this procedure; the heat map could quickly alert the clinician to the most suspicious regions requiring further exploration with the HRME. Figure 4 illustrates this approach in a patient with a floor-of-mouth lesion (Figure 4A) imaged using AFI (Figure 4B). A heat map overlay based on the RG ratio is shown in Figure 4C along with pathologic diagnoses at 6 sites. Each of the 4 sites (a, d, e, f) diagnosed as CIS was clearly highlighted by the heat map. In contrast, the sites diagnosed as mild dysplasia (c) and normal (b) were highlighted only sparsely, if at all. The correlation between the heat map and pathologic severity in this patient provides evidence for the potential usefulness of AFI for site localization. A tool capable of automatically generating AFI heat maps at the point of care and integrating the results with images obtained from the HRME could streamline risk evaluation and biopsy guidance.

Markedly hyperkeratinized lesions present perhaps the biggest limitation to multimodal imaging. As previously mentioned, clinicians using AFI must be aware that keratin itself is autofluorescent, so it is possible that dysplasia can be present in thickly keratinized lesions, even if there is no loss of fluorescence. More importantly, a superficial keratin layer can impede the ability of the HRME to image nuclei. HRME images of keratinized sites often

show keratin with no visible nuclei or sparsely distributed nuclei; it can be impossible or challenging to extract diagnostic information from these images. We hypothesize that this effect is caused by increased light scattering that limits signal from nuclei beneath the keratin layer and/or keratin acting as a physical barrier to limit proflavine penetration into the cellular layers of the epithelium. We are exploring the possibility of using a brush-like tool to manually remove a thin keratin layer at specific sites to allow for HRME imaging.

Although further work remains to be done before multimodal imaging can be recommended for widespread clinical usage, we believe that it has the potential to meet all of the diagnostic adjunct criteria that we have presented here. Initial results suggest that multimodal imaging may have high sensitivity and specificity for high-grade dysplasia and cancer.⁴⁰ Incorporating AFI allows for assessment of a large region, and the equipment is affordable and the procedure minimally invasive with few consumables required. Automated algorithms allow for obtaining immediate, objective results and reduce the need for clinical training to perform the procedure and interpret the results.

Optical coherence tomography

OCT has been successfully utilized for clinical use in certain anatomic sites, such as the coronary arteries and the esophagus, and is being actively studied for many other sites. A few groups have used OCT to image PPOELs and oral cancer. OCT produces 2-dimensional tissue cross-sections of light scattering, which are stitched together to produce a 3-dimensional volumetric map. The advantages of OCT include micron level resolution with large penetration depth (~2 mm, typically) and FOV (up to ~1 cm × 1 cm) compared with most other IVM techniques. The large penetration depth allows for visualization of the full epithelial thickness and superficial connective tissue to evaluate cellular invasion.

Recently, Lee et al.⁴¹ developed a handheld, side-looking fiber optic rotary pullback catheter placed within a sheath suitable for the oral epithelium. The device was designed to prioritize FOV and acquisition time while sacrificing resolution. It is capable of imaging an area of 90 mm × 2.5 mm with 20 to 40 μm lateral resolution in 45 seconds, with longer acquisition times improving the depth resolution. The authors acquired 176 OCT volumes of the normal mucosa, scar tissue, PPOELs with and without dysplasia, and OSCC from 51 patients. They were able to visualize architectural features, such as epithelial thickness and basement membrane continuity, and showed sample images from clinically normal tissue, leukoplakia, and submucous fibrosis. Further analysis of 31 volumes suggested that the gradient mean and gradient standard deviation of the epithelium could be used to distinguish dysplasia and OSCC from normal tissue⁴² and that this process can be automated.⁴³ Although this approach is promising, prospective studies are needed to assess and validate its potential utility for biopsy site guidance.

Wilder-Smith et al.⁴⁴ used a fiber optic high-resolution 3-dimensional OCT probe (10-mm-long scans) and a commercially available OCT system (2-mm-long scans) for in vivo imaging of the epithelium, lamina propria, and basement membrane in 50 patients with leukoplakia or erythroplakia (Figure 5). OCT images were scored by 2 pretrained, blinded individuals on a scale of 0 (normal) to 6 (OSCC), based on changes in keratin, epithelial thickness, epithelial proliferation and invasion, rete peg broadening, epithelial stratification

irregularities, and basal hyperplasia. Scorers were able to distinguish OSCC from noncancerous lesions with a sensitivity and specificity of 93.1% compared with biopsy. However, the authors did not comment on the ability to distinguish dysplastic sites from nondysplastic sites.

Tsai et al.⁴⁵ used a swept-source OCT system with a scanning speed of 10 cm/s and 1 cm scanning length to differentiate oral lesions at different stages of carcinogenesis. Lateral scan intensity profiles of the OCT images were used to differentiate between OSCC, mild and moderate dysplasia, and normal tissue. However, because of the small sample size, sensitivity and specificity were not estimated.

Although OCT has demonstrated its potential to improve the evaluation of PPOELs, further work is necessary to tailor the physical form factor and performance characteristics for defined clinical purposes. Additionally, studies with larger samples sizes and prospective algorithm evaluation are required to validate diagnostic accuracy in vivo.

Reflectance confocal microscopy

In reflectance confocal microscopy (RCM), a pinhole is used to reject out-of-focus light that has been reflected from the sample. The pinhole improves resolution and allows for obtaining images of various depths of tissue and for potential differentiation of different grades of dysplasia. With the exception of hypertrophic lesions, RCM systems may be configured to image the basement membrane and superficial connective tissue.

Olsovsky et al.⁴⁶ developed a handheld RCM endomicroscope with an electrically tunable lens and a double-clad fiber coupler to obtain 850 μm diameter in vivo images of oral lesions at depths of up to 250 μm with 1.7- μm lateral resolution and 6- to 12- μm depth resolution. The endomicroscope form factor allows for imaging of hard-to-reach areas of the mouth. The imaging procedure consists of first applying 5% acetic acid to the mucosa, followed by a 5-second acquisition time. Olsovsky et al. showed images of the normal oral mucosa (Figures 6A–6C), leukoplakia of the buccal mucosa containing mild to focally moderate dysplasia (Figures 6D–6H), and ulcerated granulation tissue with chronic inflammation at various depths. They were able to visualize cellular and nuclear morphology associated with inflammation and dysplasia. Additionally, they have developed an automated algorithm capable of nuclear segmentation of RCM images.⁴⁷

They have also developed a fluorescence lifetime imaging (FLIM) system capable of imaging a 1.6×1.6 cm area.⁴⁸ FLIM measures tissue autofluorescence, similar to AFI, but it also provides information about fluorescence decay as a function of time, potentially enabling estimates of the contribution of specific fluorophores, such as NADH, FAD, and collagen. They hypothesized that the additional information may be helpful in distinguishing dysplastic lesions from benign inflammatory lesions and proposed a multiscale approach similar to our own, consisting of FLIM imaging followed by RCM at high-risk sites identified by FLIM. So far, 4 biopsy specimens have been imaged ex vivo by using this approach, with qualitative and quantitative differences observed between normal, benign, and SCC tissues.⁴⁹ An in vivo study is currently underway.

Multiphoton microscopy

Similar to confocal imaging, multiphoton microscopy is a type of fluorescence imaging that can obtain image cross-sections at various depths of tissues, at large depths of up to 1 mm. The large penetration depth could potentially enable evaluation of cellular invasion past the basement membrane. In multiphoton microscopy, the excitation light source uses light with twice the desired fluorescence excitation wavelength so that fluorescence occurs only when 2 photons excite a fluorophore simultaneously. This process only occurs with significant frequency at a narrow point. The absence of out-of-focus fluorescence absorption allows the excitation light source to penetrate deeper into tissue, and the longer wavelengths used for excitation decrease scattering effects. Autofluorescence-based multiphoton microscopy measures the same signals as existing AFI instrumentation, but with the added advantage of depth-sectioned visualization of microscopic features. However, multiphoton microscopy instruments can typically only image FOV of a few hundred microns in diameter and require much stronger light intensity.

Multiphoton microscopy approaches have been studied in a variety of cancer types, providing a basis for its potential use in oral dysplasia and cancer. Matsui et al.⁵⁰ used multiphoton autofluorescence microscopy to image epithelial cells, immune cells, and basement membrane in human colorectal mucosa by using emission peaks from NADH, nicotinamide adenine dinucleotide phosphate, FAD, and collagen. The authors were able to classify 64 normal and 80 cancerous tissue specimens by using nuclear diameter and collagen intensity, with 96% sensitivity and 84% specificity.

Pal et al.⁵¹ reported the use of multiphoton autofluorescence microscopy in a hamster model of oral neoplasia. They were able to visualize cytoplasm, nuclei, and keratin at a depth of 30 μm in the epithelium and identified emission peaks for the same epithelial fluorophores (NADH, FAD, and protoporphyrin IX) that contribute to AFI signal. Sensitivity and specificity for the identification of neoplasia were not evaluated, and images at depths other than 30 μm were not obtained. Significant technical advances are necessary before in vivo use of multiphoton autofluorescence microscopy will be feasible, although its use on ex vivo human specimens or in animal models could advance scientific understanding of autofluorescence of the oral mucosa.

CONCLUSIONS

Improved methods to diagnose and risk-stratify PPOELs could decrease the global burden of oral cancers. Biopsy is the gold standard for diagnosing dysplasia and cancer, but it is limited by morbidity, time and resource requirements, and the risk of sampling bias. The existing diagnostic adjuncts that provide immediate feedback are limited by poor diagnostic accuracy. In vivo microscopy technologies are a promising avenue to help clinicians identify high-risk PPOELs and select a biopsy site, which could result in improved patient care. However, additional technology development and clinical studies are required to establish and validate their diagnostic accuracy and use.

Acknowledgments

This work was supported by National Institutes of Health grants R01 CA103830 (to R. Richards-Kortum); R01 CA185207 (to R. Richards-Kortum); R01 DE024392 (to N. Vigneswaran); F30 CA213922 (to E. Yang); and by the Cancer Prevention and Research Institute of Texas (CPRIT) grant RP100932 (to R. Richards-Kortum).

The authors thank current and former personnel at Rice University, M.D. Anderson Cancer Center, and University of Texas School of Dentistry for their contributions: Katelin Cherry and Imran Vohra (Rice University); Hawraa Badaoui, Jessica Rodriguez and Michelle D. Williams (M.D. Anderson Cancer Center); Alexander Lang and Nancy Bass (University of Texas School of Dentistry).

References

1. Ferlay J, Soerjomataram I, Dikshit R, et al. Cancer incidence and mortality worldwide: sources, methods and major patterns in GLOBOCAN 2012. *Int J Cancer*. 2015; 136:E359–E386. [PubMed: 25220842]
2. Warnakulasuriya S. Global epidemiology of oral and oropharyngeal cancer. *Oral Oncol*. 2009; 45:309–316. [PubMed: 18804401]
3. Warnakulasuriya S, Johnson NW, Van Der Waal I. Nomenclature and classification of potentially malignant disorders of the oral mucosa. *J Oral Pathol Med*. 2007; 36:575–580. [PubMed: 17944749]
4. Warnakulasuriya S, Ariyawardana A. Malignant transformation of oral leukoplakia: a systematic review of observational studies. *J Oral Pathol Med*. 2016; 45:155–166. [PubMed: 26189354]
5. Bouquot JE, Speight PM, Farthing PM. Epithelial dysplasia of the oral mucosa—diagnostic problems and prognostic features. *Curr Diagn Pathol*. 2006; 12:11–21.
6. Mehanna HM, Rattay T, Smith J, McConkey CC. Treatment and follow-up of oral dysplasia—a systematic review and meta-analysis. *Head Neck*. 2009; 31:1600–1609. [PubMed: 19455705]
7. Barnes L, Eveson JW, Reichart P, Sidransky D. World Health Organization Classification of Tumours. 9. Lyon, France: IARC Press; 2005. Tumours of the oral cavity and oropharynx; 178
8. Reibel J. Prognosis of oral pre-malignant lesions: significance of clinical, histopathological, and molecular biological characteristics. *Crit Rev Oral Biol Med*. 2003; 14:47–62. [PubMed: 12764019]
9. Brennan JA, Mao L, Hruban RH, et al. Molecular assessment of histopathological staging in squamous-cell carcinoma of the head and neck. *N Engl J Med*. 1995; 332:429–435. [PubMed: 7619114]
10. Mao L, Papadimitrakopoulou V, Shin DM, et al. Phenotype and genotype of advanced premalignant head and neck lesions after chemopreventive therapy. *JNCI J Natl Cancer Inst*. 1998; 90:1545–1551. [PubMed: 9790547]
11. William WN, Papadimitrakopoulou V, Lee JJ, et al. Erlotinib and the risk of oral cancer. *JAMA Oncol*. 2016; 2:209. [PubMed: 26540028]
12. Patel KJ, De Silva HL, Tong DC, Love RM. Concordance between clinical and histopathologic diagnoses of oral mucosal lesions. *J Oral Maxillofac Surg*. 2011; 69:125–133. [PubMed: 20971541]
13. Seoane J, Warnakulasuriya S, Varela-Centelles P, Esparza G, Dios P. Oral cancer: experiences and diagnostic abilities elicited by dentists in North-western Spain. *Oral Dis*. 2006; 12:487–492. [PubMed: 16910920]
14. Epstein JB, Güneri P, Boyacioglu H, Abt E. The limitations of the clinical oral examination in detecting dysplastic oral lesions and oral squamous cell carcinoma. *J Am Dent Assoc*. 2012; 143:1332–1342. [PubMed: 23204089]
15. Forman MS, Chuang S-K, August M. The accuracy of clinical diagnosis of oral lesions and patient-specific risk factors that affect diagnosis. *J Oral Maxillofac Surg*. 2015; 73:1932–1937. [PubMed: 25981860]
16. Goodson M, Kumar A, Thomson P. P171. Oral precancer excision is required for definitive diagnosis: incisional vs excisional biopsies in oral leukoplakia management. *Oral Oncol*. 2011; 47:S128–S129.

17. Chen S, Forman M, Sadow PM, August M. The diagnostic accuracy of incisional biopsy in the oral cavity. *J Oral Maxillofac Surg.* 2016; 74:959–964. [PubMed: 26682520]
18. Lee J-J, Hung H-C, Cheng S-J, et al. Factors associated with underdiagnosis from incisional biopsy of oral leukoplakic lesions. *Oral Surg Oral Med Oral Pathol Oral Radiol Endod.* 2007; 104:217–225.
19. Speight PM. Update on oral epithelial dysplasia and progression to cancer. *Head Neck Pathol.* 2007; 1:61–66. [PubMed: 20614284]
20. Speight PM, Abram TJ, Floriano PN, et al. Interobserver agreement in dysplasia grading: toward an enhanced gold standard for clinical pathology trials. *Oral Surg Oral Med Oral Pathol Oral Radiol.* 2015; 120:474–482. e2. [PubMed: 26216170]
21. El-Naggar A, Chan J, Grandis J, Takata T, Slootweg P. WHO Classification of Head and Neck Tumours. 4. Lyon, France: IARC Press; 2017.
22. Lingen MW, Abt E, Agrawal N, et al. Evidence-based clinical practice guideline for the evaluation of potentially malignant disorders in the oral cavity. *J Am Dent Assoc.* 2017; 148:712–727. [PubMed: 28958308]
23. Lingen MW, Kalmar JR, Karrison T, Speight PM. Critical evaluation of diagnostic aids for the detection of oral cancer. *Oral Oncol.* 2008; 44:10–22. [PubMed: 17825602]
24. Macey R, Walsh T, Brocklehurst P, et al. Diagnostic tests for oral cancer and potentially malignant disorders in patients presenting with clinically evident lesions. *Cochrane Database Syst Rev.* 2015; (5) CD010276.
25. Sridharan G, Shankar AA. Toluidine blue: a review of its chemistry and clinical utility. *J Oral Maxillofac Pathol.* 2012; 16:251–255. [PubMed: 22923899]
26. Mehrotra R, Singh M, Thomas S, et al. A cross-sectional study evaluating chemiluminescence and autofluorescence in the detection of clinically innocuous precancerous and cancerous oral lesions. *J Am Dent Assoc.* 2010; 141:151–156. [PubMed: 20123872]
27. Farah CS, McCullough MJ. A pilot case control study on the efficacy of acetic acid wash and chemiluminescent illumination (ViziLite) in the visualisation of oral mucosal white lesions. *Oral Oncol.* 2007; 43:820–824. [PubMed: 17169603]
28. Poh CF, Zhang L, Anderson DW, et al. Fluorescence visualization detection of field alterations in tumor margins of oral cancer patients. *Clin Cancer Res.* 2006; 12:6716–6722. [PubMed: 17121891]
29. Poh CF, Anderson DW, Durham JS, et al. Fluorescence visualization-guided surgery for early-stage oral cancer. *JAMA Otolaryngol Neck Surg.* 2016; 142:209.
30. Pavlova I, Williams M, El-Naggar A, Richards-Kortum R, Gillenwater A. Understanding the biological basis of autofluorescence imaging for oral cancer detection: high-resolution fluorescence microscopy in viable tissue. *Clin Cancer Res.* 2008; 14:2396–2404. [PubMed: 18413830]
31. Adhi M, Duker JS. Optical coherence tomography—current and future applications. *Curr Opin Ophthalmol.* 2013; 24:213–221. [PubMed: 23429598]
32. Bezerra HG, Costa MA, Guagliumi G, Rollins AM, Simon DI. Intracoronary optical coherence tomography: a comprehensive review. *JACC Cardiovasc Interv.* 2009; 2:1035–1046. [PubMed: 19926041]
33. Canto MI, Anandasabapathy S, Brugge W, et al. In vivo endomicroscopy improves detection of Barrett's esophagus-related neoplasia: a multicenter international randomized controlled trial. *Gastrointest Endosc.* 2014; 79:211–221. [PubMed: 24219822]
34. Stevenson AD, Mickan S, Mallett S, Ayya M. Systematic review of diagnostic accuracy of reflectance confocal microscopy for melanoma diagnosis in patients with clinically equivocal skin lesions. *Dermatol Pract Concept.* 2013; 3:19–27. [PubMed: 24282659]
35. Muldoon TJ, Pierce MC, Nida DL, Williams MD, Gillenwater A, Richards-Kortum R. Subcellular-resolution molecular imaging within living tissue by fiber microendoscopy. *Opt Express.* 2007; 15:16413–16423. [PubMed: 19550931]
36. Quang T, Schwarz RA, Dawsey SM, et al. Atablet-interfaced high-resolution microendoscope with automated image interpretation for real-time evaluation of esophageal squamous cell neoplasia. *Gastrointest Endosc.* 2016; 84:834–841. [PubMed: 27036635]

37. Shin D, Pierce MC, Gillenwater AM, Williams MD, Richards-Kortum RR. A fiber-optic fluorescence microscope using a consumer-grade digital camera for *in vivo* cellular imaging. *PLoS ONE*. 2010; 5:e11218. [PubMed: 20585636]
38. Koucky MH, Pierce MC. Axial response of high-resolution microendoscopy in scattering media. *Biomed Opt Express*. 2013; 4:2247. [PubMed: 24156080]
39. Roblyer D, Kurachi C, Stepanek V, et al. Objective detection and delineation of oral neoplasia using autofluorescence imaging. *Cancer Prev Res (Phila)*. 2009; 2:423–431. [PubMed: 19401530]
40. Pierce MC, Schwarz RA, Bhattar VS, et al. Accuracy of *in vivo* multimodal optical imaging for detection of oral neoplasia. *Cancer Prev Res (Phila)*. 2012; 5:801–809. [PubMed: 22551901]
41. Lee AM, Cahill L, Liu K, MacAulay C, Poh C, Lane P. Wide-field *in vivo* oral OCT imaging. *Biomed Opt Express*. 2015; 6:2664–2674. [PubMed: 26203389]
42. Raizada R, Lee AMD, Liu KY, et al. Wide-field OCT imaging of oral lesions *in vivo*: quantification and classification [conference paper]. In: Wong B, Ilgner J, Izdebski K, editors *Optical Imaging, Therapeutics, and Advanced Technology in Head and Neck Surgery and Otolaryngology*. Vol. 10039. San Francisco, California, USA: SPIE BiOS; 2017. Proceedings, 100390 G (2017).
43. Goldan RN, Lee A, Cahill LC, et al. Advanced Biomedical and Clinical Diagnostic and Surgical Guidance Systems XIV. Vol. 9698. San Francisco, California, USA: SPIE BiOS; 2016. Automated 3 D segmentation of oral mucosa from wide-field OCT images [conference paper]. Proceedings, 96980R (2016).
44. Wilder-Smith P, Lee K, Guo S, et al. *In vivo* diagnosis of oral dysplasia and malignancy using optical coherence tomography: Preliminary studies in 50 patients. *Lasers Surg Med*. 2009; 41:353–357. [PubMed: 19533765]
45. Tsai M-T, Lee C-K, Lee H-C, et al. Differentiating oral lesions in different carcinogenesis stages with optical coherence tomography. *J Biomed Opt*. 2009; 14:44028.
46. Olsovsky C, Hinsdale T, Cuenca R, et al. Handheld tunable focus confocal microscope utilizing a double-clad fiber coupler for *in vivo* imaging of oral epithelium. *J Biomed Opt*. 2017; 22:56008. [PubMed: 28541447]
47. Harris MA, Van AN, Malik BH, Jabbour JM, Maitland KC. Apulse coupled neural network segmentation algorithm for reflectance confocal images of epithelial tissue. *PLoS ONE*. 2015; 10:e0122368. [PubMed: 25816131]
48. Cheng S, Cuenca RM, Liu B, et al. Handheld multispectral fluorescence lifetime imaging system for *in vivo* applications. *Biomed Opt Express*. 2014; 5:921. [PubMed: 24688824]
49. Malik BH, Jabbour JM, Cheng S, et al. A novel multimodal optical imaging system for early detection of oral cancer. *Oral Surg Oral Med Oral Pathol Oral Radiol*. 2016; 121:290–300. e2. [PubMed: 26725720]
50. Matsui T, Mizuno H, Sudo T, et al. Non-labeling multiphoton excitation microscopy as a novel diagnostic tool for discriminating normal tissue and colorectal cancer lesions. *Sci Rep*. 2017; 7:6959. [PubMed: 28761050]
51. Pal R, Edward K, Ma L, Qiu S, Vargas G. Spectroscopic characterization of oral epithelial dysplasia and squamous cell carcinoma using multiphoton autofluorescence micro-spectroscopy. *Lasers Surg Med*. 2017; 49:866–873. [PubMed: 28677822]

Statement of Clinical Relevance

Existing methods to evaluate potentially premalignant oral epithelia lesions often lead to suboptimal diagnosis and management, increasing the global oral cancer burden. Novel in vivo microscopy technologies allow clinicians to visualize microscopic tissue features at the point of care to facilitate evidence-based patient care.

Author Manuscript

Author Manuscript

Author Manuscript

Author Manuscript

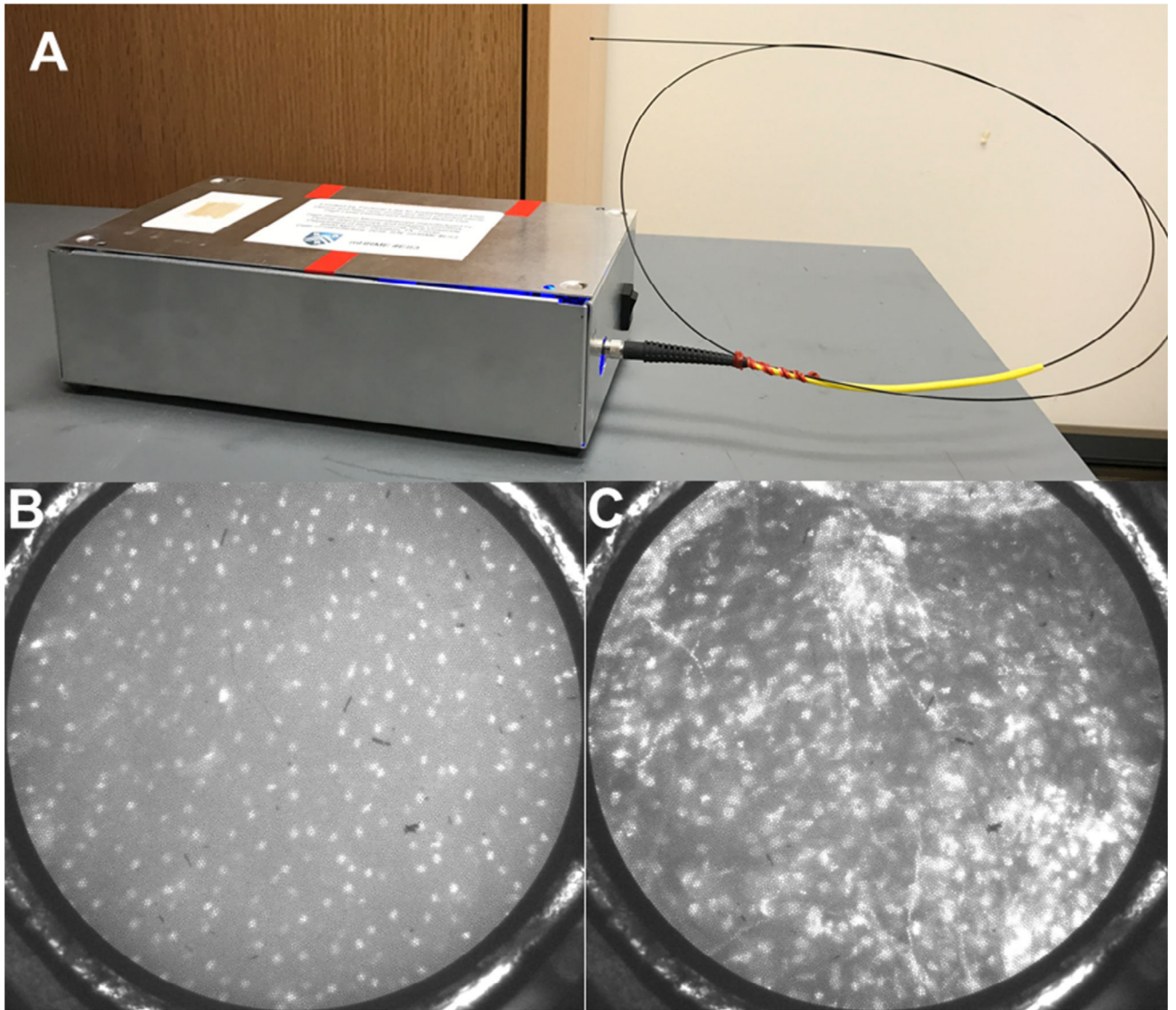


Fig. 1. High-resolution microendoscopy. **A**, Photo of the high-resolution microendoscope (HRME) with attached probe. HRME images of histopathologically diagnosed **(B)** normal oral mucosa showing small, evenly spaced nuclei and **(C)** severe dysplasia showing enlarged, crowded nuclei. Field of view is 0.79 mm in diameter.

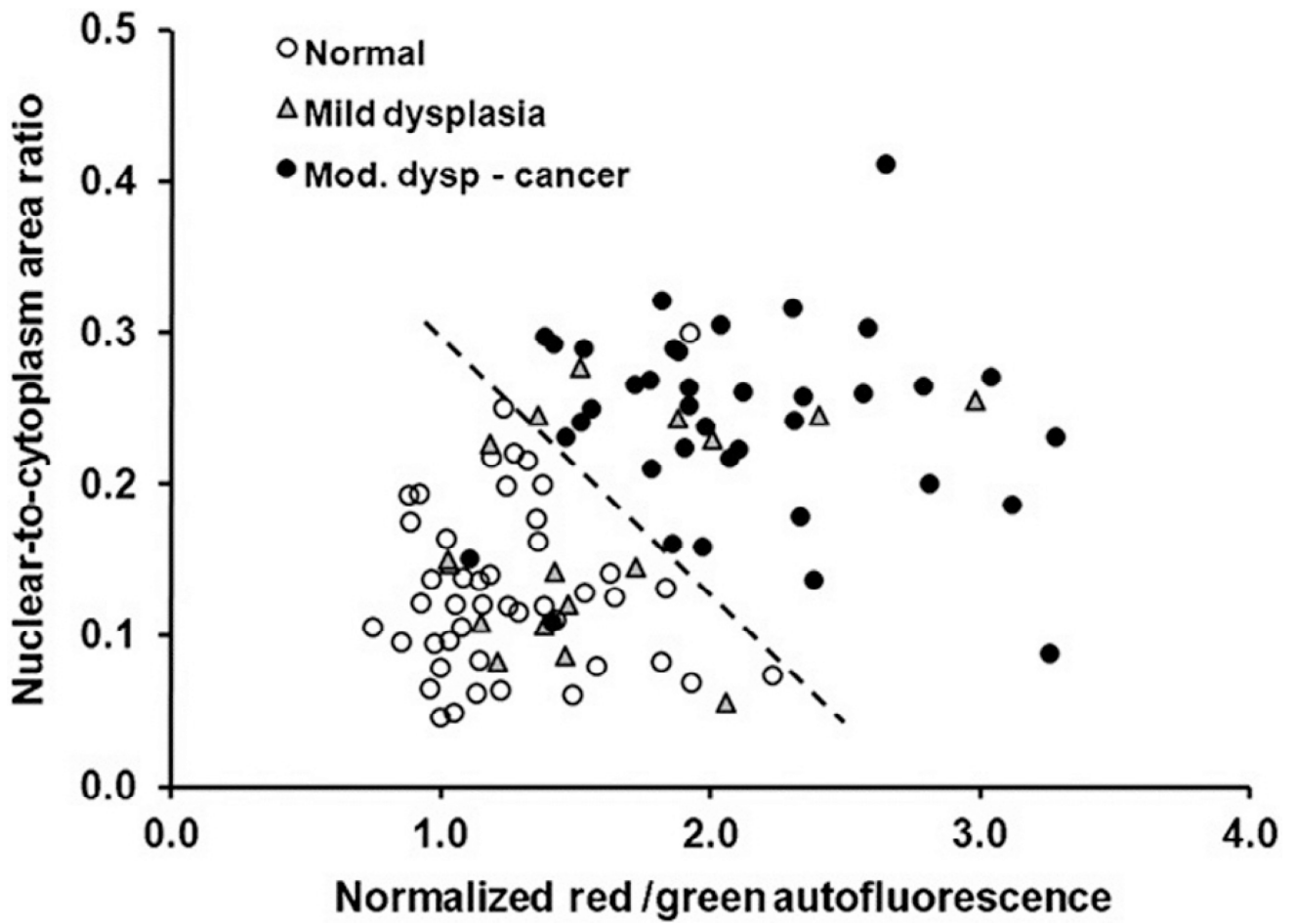


Fig. 2. Classification of imaged sites based on autofluorescence imaging and high-resolution microendoscope (HRME). The dashed line represents a linear threshold to distinguish normal sites from moderate dysplasia to cancer sites based on imaging metrics. (Reprinted from Pierce et al.⁴⁰).

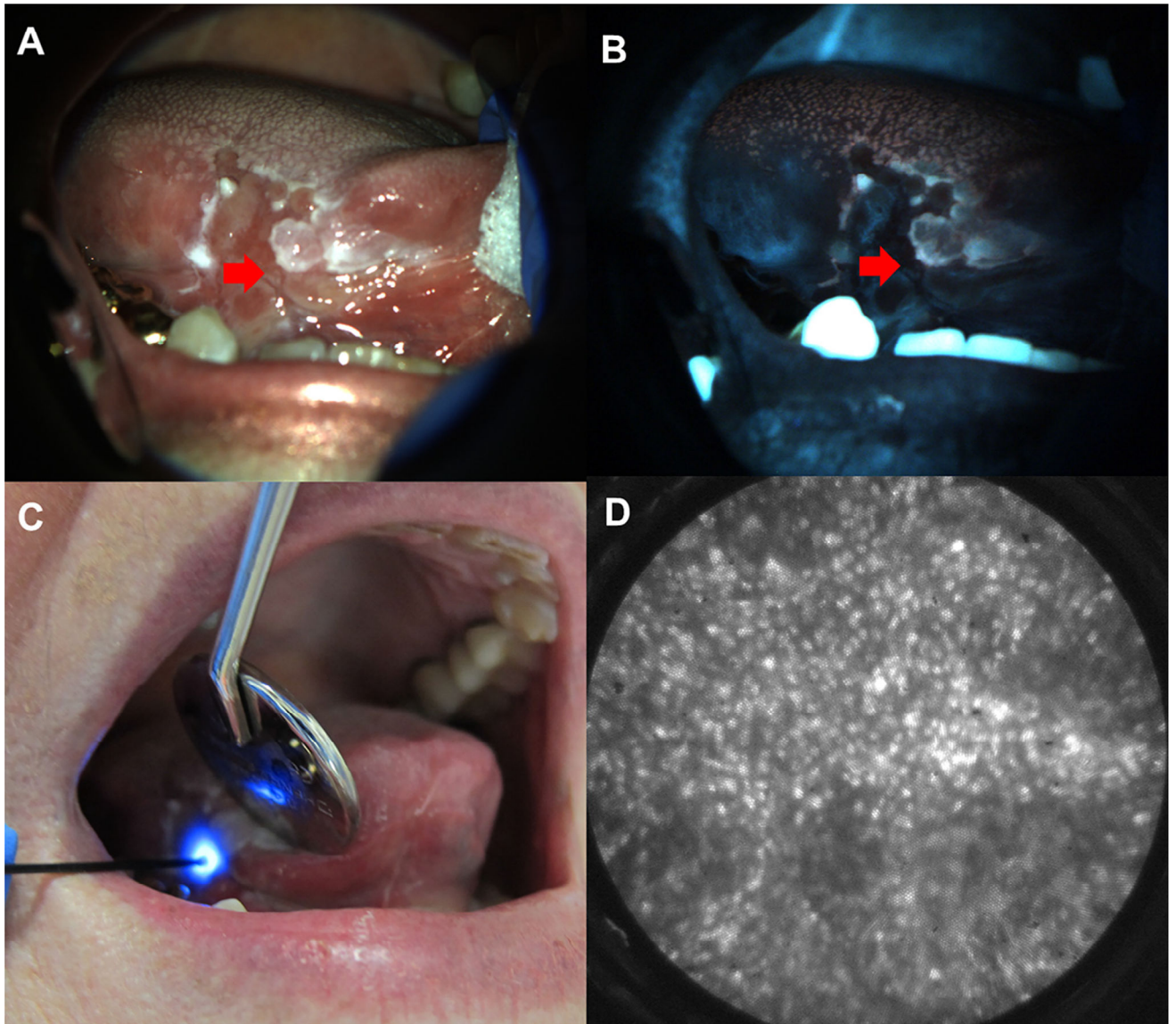


Fig. 3. Multimodal imaging example. White light (A) and autofluorescence image (B) of red and white ulcerated lesion on the right lateral tongue in a 75-year-old female presenting at the University of Texas School of Dentistry. Site imaged with HRME (red arrow) showed loss of fluorescence with elevated normalized red-green ratio. (C) HRME probe on imaged site. (D) HRME image at site showed enlarged, crowded nuclei. Biopsy of the site was performed, and pathologic diagnosis was invasive OSCC.

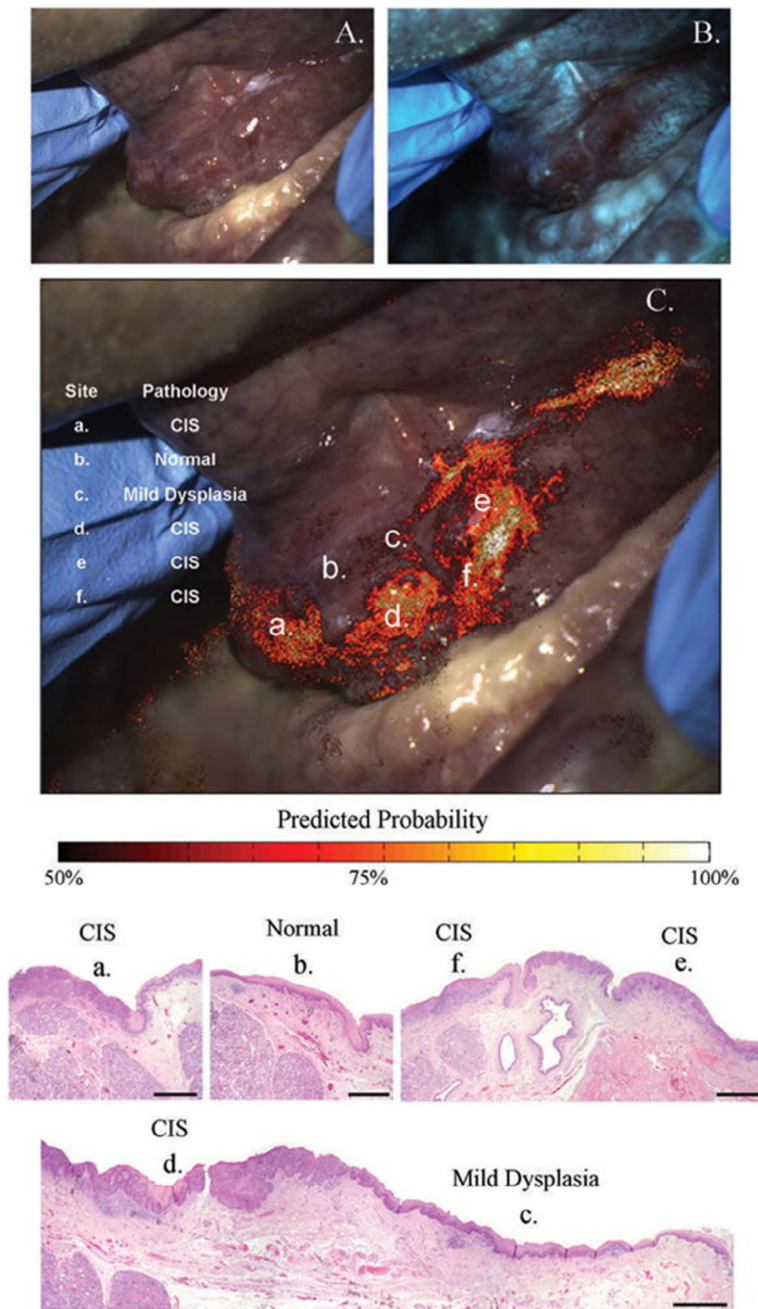


Fig. 4. Risk heat map based on autofluorescence imaging. White light (**A**) and autofluorescence image (**B**) of floor of mouth lesion containing histopathologically confirmed dysplasia and carcinoma in situ. **C**, Risk heat map based on red-green ratio overlaid on white light image, with pathologic diagnoses at 6 sites denoted by lowercase letters (a–f). Histology slides of the six sites are shown below (scale bar = 1 mm). (Reprinted from Roblyer et al.³⁹).

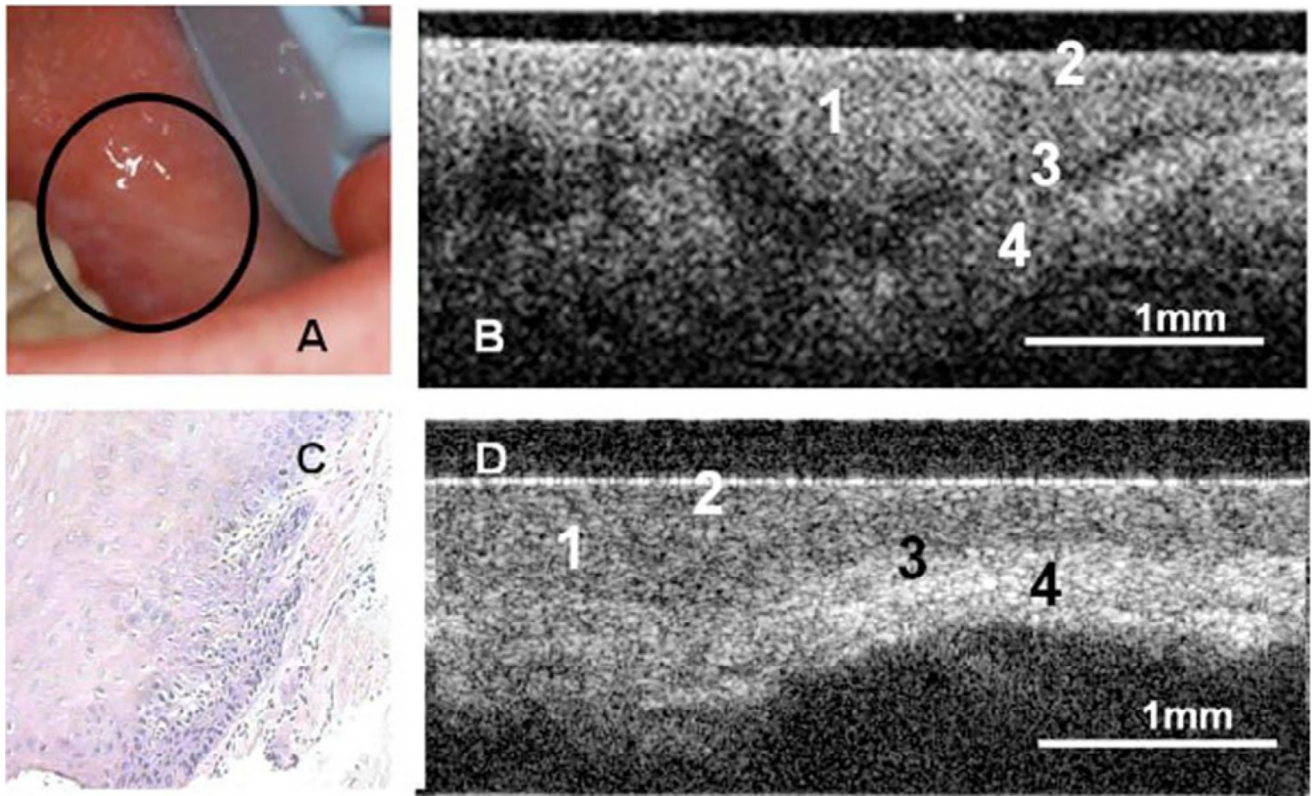


Fig. 5. Optical coherence tomography (OCT) in the oral mucosa. **A–C**, Photograph (**A**), in vivo OCT image (**B**), and $\times 10$ hematoxylin and eosin (H&E slide) (**C**) of dysplastic buccal mucosa. **D**, In vivo OCT image of normal buccal mucosa: (1) stratified squamous epithelium, (2) keratinized epithelial surface layer, (3) basement membrane, (4) submucosa. (Reprinted with permission from Wilder-Smith et al.⁴⁴).

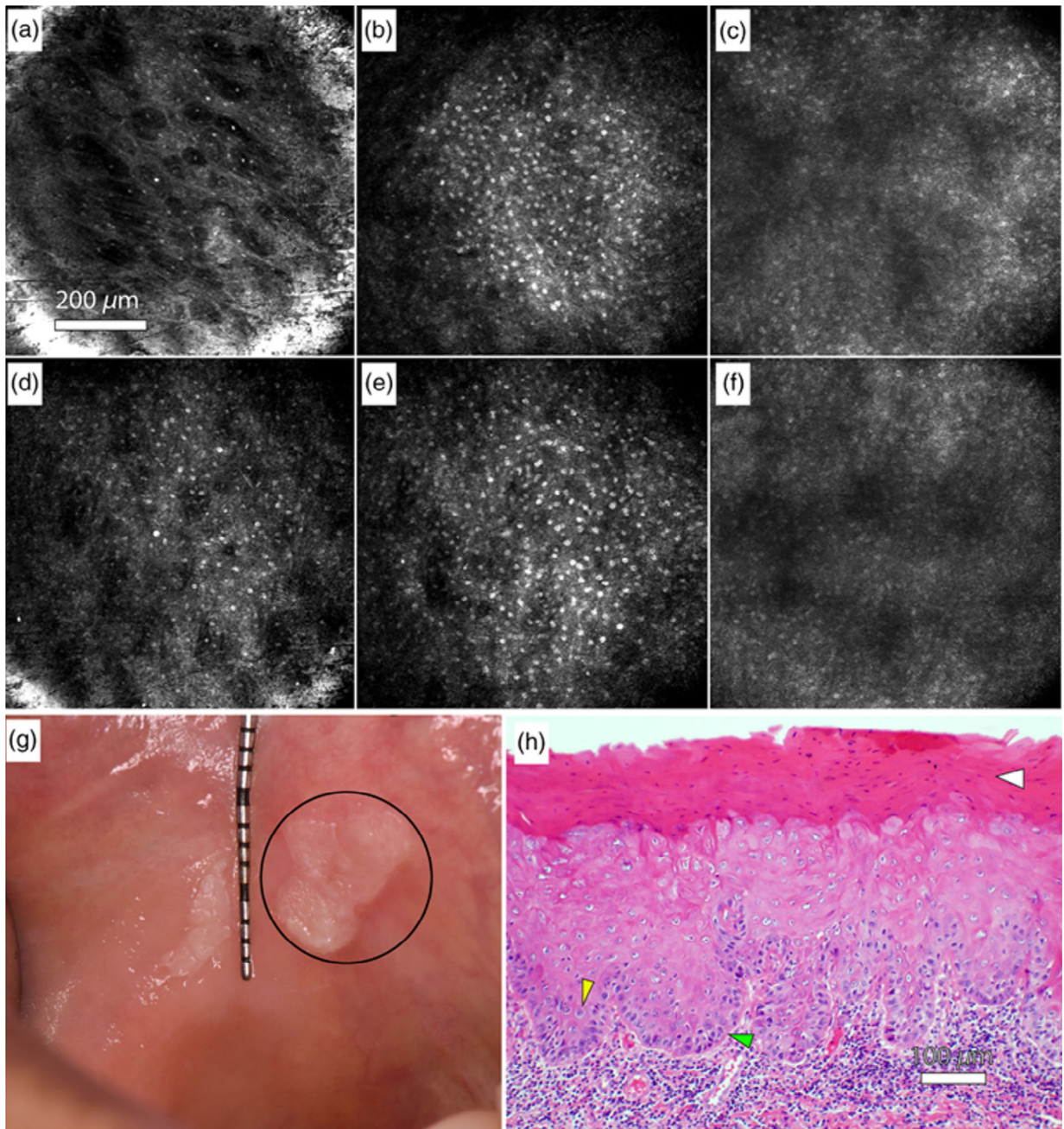


Fig. 6. Reflectance confocal microscopy in the oral mucosa. **A–C**, In vivo reflectance confocal microscopy images of clinically normal buccal mucosa at depths of approximately **(A)** 10 μm (superficial epithelium), **(B)** 70 μm (spinous layer), and **(C)** 120 μm (approaching basement membrane). **D–F**, In vivo reflectance confocal microscopy images of a leukoplakia at depths of approximately **(D)** 10 μm (superficial epithelium), **(E)** 70 μm (spinous layer), and **(F)** 120 μm (approaching basement membrane). **G**, Photograph of the leukoplakia, including the imaged lesion (*circle*). **H**, Hematoxylin and eosin (**H&E**) slide of imaged leukoplakia diagnosed as mild to focally moderate dysplasia. Yellow arrow: Increased

nuclear to cytoplasmic ratio. Green arrow: Loss of polarity of basal cells. White arrow: Hyperkeratosis. (Reprinted from Olsovsky et al.⁴⁶).

Author Manuscript

Author Manuscript

Author Manuscript

Author Manuscript

Table I

Limitations of biopsy

Sampling bias as a result of site selection
Trained clinician required to perform biopsy correctly
Trained pathologist and processing facilities required for diagnosis
Lengthy time (days) to diagnosis
Interobserver and intraobserver variance
Patient morbidity and discomfort

Author Manuscript

Author Manuscript

Author Manuscript

Author Manuscript

Existing diagnostic adjuncts

Table II

Technique	Sensitivity	Specificity	Time to result	Size of area assessed	Cost	Training required	Invasiveness	Objective interpretation
Biopsy	Gold standard	Gold standard	Days	Small	High	High	High	No
Cytology/brush biopsy	High	High	Days	Small	Medium	Medium	Moderate	Partially
Toluidine blue	OSCC: High Dysplasia: Low	Low	Immediate	Large	Low	Medium	Minimal	No
Acetowhitening/chemiluminescence	Low	Low	Immediate	Large	Medium	Medium	Minimal	No
Autofluorescence imaging	High	Low	Immediate	Large	Medium	Medium	None	No, but potentially yes

OSCC, oral squamous cell carcinoma.

Table III

Effects of tissue changes on autofluorescence

Histologic assessment	Autofluorescence feature
Epithelial hyperplasia	No change
Dysplasia	Complete or partial loss
Invasive carcinoma	Complete loss
Verruciform hyperkeratosis	No change or increase
Infectious	Complete or partial loss
Vascular lesions	Complete or partial loss
Submucous fibrosis	Enhanced
Amalgam pigmentation (tattoo)	Complete loss
Focal melanosis	Complete loss
Hairy leukoplakia / candidiasis	Red to orange spectrum

Adapted with permission from Vigneswaran and El-Naggar. Early detection and diagnosis of oral premalignant squamous mucosal lesions. In: Wong BJ, Ilgner J, eds. *Biomedical Optics in Otorhinolaryngology*. New York: Springer; 2016:601–618.

Author Manuscript

Author Manuscript

Author Manuscript

Author Manuscript

Table IV

IVM adjuncts under development

Technique	Sensitivity	Specificity	Time to result	Size of area assessed	Cost	Invasiveness	Objective interpretation
Multimodal imaging	Potentially high	Potentially high	Immediate	Large	Medium	Minimal	Potentially
Optical coherence tomography	TBD	TBD	Immediate	Medium	High	Minimal	Potentially
FLIM + RCM	TBD	TBD	Immediate	Medium	High	Minimal	Potentially
Multiphoton microscopy	TBD	TBD	Immediate	Small	High	Minimal	Potentially

FLIM, fluorescence lifetime imaging; *IVM*, in vivo microscopy; *RCM*, reflectance confocal microscopy; *TBD*, to be determined.